Chapter 5
Signals with an Additive Fractal Structure for Information Transmission

M. V. Kapranov
Moscow Power Engineering Institute, Russia

A. V. Khandurin
Moscow Power Engineering Institute, Russia

ABSTRACT

This chapter is devoted to a new class of wideband signals with an additive fractal structure. Properties and characteristics of the new type of signals are studied. It is shown that such signals possess a high level of an irregularity and unpredictability at simple technical implementation. It is shown that an incommensurability of frequencies of fundamental high-stable oscillations leads to the high level of an irregularity of such signals. For an estimation of a level of signal complexity, authors offer to use the fractal dimensionality of their temporal implementations calculated by means of creation of the structural function. Methods of modification of the signal spectrum with the additive fractal structure are offered, permitting to increase the efficiency of the frequency resource application. For reduction of the high low-frequency signal power the authors suggest using signals with the additive fractal structure, centered in a moving average window. Methods of masking of the voice messages by means of signals of a new type are offered. The results of a computer experiment of secretive sound transmission are described.

INTRODUCTION

In the present time there are some important problems of information transfer through radio channels – the electromagnetic compatibility, an increase of data capacity of carrier oscillations, the security and stealthiness of communication. One of the methods of solution of the mentioned problems is based on the reduction of the power spectral density of the message under transmission, at the expense of the extension of its frequency band. Thus in classical methods of the spectrum

DOI: 10.4018/978-1-4666-2208-1.ch005

extension (Ipatov, 2007), the sophisticated modulation of clean waves (CW) is used that leads to serious complication of transmitters and receivers.

Without application of technology of the spectrum extension the specified problems can be solved using non-sinusoidal waves, but the wideband carrier signals. Nowadays there is a tendency to use signals on the basis of a dynamic chaos (Pecora & Carroll, 1990, pp.821-824; Cuomo & Oppenheim, 1993, pp.65-68; Kuznetsov, 2000) as carrier oscillations. However, application of chaotic signals in communication systems (Dedieu, Kennedy, & Hasler, 1993, pp.634-642; Kapranov & Morozov, 1998, pp.66-71; Murali & Leung & Yu, 2003, pp.432-441; Yang, 2004, pp.81-130) has revealed two large lacks. Firstly, the complex nonlinear mechanisms of dynamic chaos formation are rather sensitive to inevitable, even insignificant, mismatches of parameters on the reception and transmission ends that lead to the impossibility of correlative processing of chaotic signals in the receiver. Secondly, it is impossible to change the structure of the chaotic carrier spectrum for adaptation to a spectrum of the message or to interference in the communication channel – the chaos characteristics are completely predetermined by a structure of the forming dynamic system and a choice of its parameters. Signals with the fractal structure are an alternative of chaotic oscillations. Fractal signals are as irregular as chaotic signals, but can give benefits on reproducibility and flexibility of characteristic change.

The subject of this chapter is a research and performance evaluation of wideband signal application with an additive fractal structure for the stealthiness transmission of analog voice messages. At first, we select the type of fractal functions for the simplest generation of signals with fractal structure on their basis, and the properties of these functions are researched. Further, from mathematical record of fractal functions, we turn to their engineering interpretation for radio signal generation. Shortcomings of fractal radio signals come to light. For the elimination of these lacks we enter signals with the modified fractal structure. In the last paragraph methods of information transmission by means of new fractal signals are offered, and the computer experiment of secured voice message transmission is carried out.

MAIN CHARACTERISTICS OF FRACTAL FUNCTIONS WITH AN ADDITIVE STRUCTURE

Signals with a fractal structure can be divided into some types according to methods of their formation in the transmitter: signals with additive (Wornell, 1996, Falconer, 1997) and multiplicative (Bolotov & Tkach, 2006, pp.91-98) structure, signals on the basis of iterative fractal functions (Kravchenko, Perez-Meana, & Ponomaryov, 2009) (functions of Cantor, Bolzano, Bezikovich, etc.), solution of nonlinear dynamic systems in the reverse time (Tomashevsky & Kapranov, 2006). The main lack of almost all fractal signals is the impossibility of their generation in the form of self-oscillations in devices with the simple structure. However, fractal functions with an additive structure and signals on their basis, which are a sum of stable sinusoidal oscillations with incommensurable frequencies, can be obtained without the expensive equipment. Except fractal properties and simple generation methods, signals with an additive fractal structure demonstrate a high level of reproducibility. These properties can be used for secured telecommunications, therefore, the research of such signals is urgent and this chapter is devoted only to them.

On determination (for example Wornell (1996)), any fractal function should satisfy the following scaling equation:

$$f\left(x\right) = \frac{1}{\mu} f\left(\lambda x\right) \tag{1}$$

Usually (Falconer, 1997, Bolotov & Tkach, 2006, pp.91-98, Kravchenko & Perez-Meana &

Ponomaryov, 2009, Tomashevsky & Kapranov, 2006, Gluzman & Sornette, 2002) for (1) examination one can search the solution in the form of the infinite additive power series:

$$f(x)=\sum_{k=1}^{\infty}\frac{1}{\mu^k}g\left[\lambda^k x\right].$$

It is possible to select any function as *g(x)*, however, from the engineering point of view, the simplest way is to form the harmonic oscillations *g(x)=sin(x)*. For the first time, a scale-invariant function with such a basis was offered by Weierstrass (Du Bois & Reymond, 1875, pp.21-37) at the end of the 19th Century.

Falkoner (1997) investigated the Weierstrass function having selected $\mu=\lambda^{(2-D)}$,

$$W(t)=\sum_{k=1}^{\infty}\lambda^{(D-2)k}\sin\left(\lambda^k t\right), \qquad (2)$$

and he has proved that at $1<D<2$, $\lambda>1$ the value of parameter D numerically corresponds to box dimension of the $W(t)$ graph. Here we obtain:

$$A_k=\lambda^{(D-2)k},\ \nu_k=\lambda^k/2\pi$$

are the amplitude and the frequency of the *k*-th component of the function accordingly.

The fractal function (2) possesses the following characteristics:

- **Nondifferentiability:** The nonregular character of behavior of the temporal implementation does not change at reduction of its scale,
- **Fractal dimension of graphs of temporal implementations:** The higher dimension leads to the higher amplitude of fast-changing components (Figure 1(a)),
- **Scale invariance:** The function completely repeats itself on small and big time scales (Figure 1(b)),
- A spectrum decaying in inverse proportion to frequency (Figure 2).

From Expression (2) it is observable that with increasing of fractal dimension D the high-frequency amplitudes of spectral components in-

Figure 1. (a) Change of a type of temporal implementation depending on its fractal dimension and (b) an illustration of self-similarity of graphs of Weierstrass function at λ=1.2

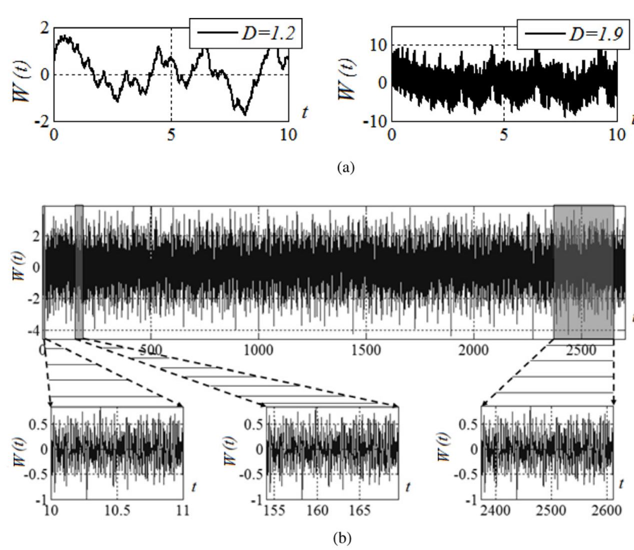

crease as well. In a limit at $D \to 2$ amplitudes of all spectral components are identical (Figure 2).

It is easy to prove the scale invariance of the Weierstrass function (see Box 1).

That is, on an abscissa axis the scale factor is equal to λ, and on an axis of ordinates - $\lambda^{(2-D)}$. The Weierstrass function repeats itself on time intervals $t_0\lambda^n \le t \le (t_0+\Delta t)\lambda^n$, (Figure 1 (b)), where $n=0\ldots\infty$ - a scaling coefficient.

When one speaks about an ergodicity of the temporal process, he implies that its statistical characteristics on the big interval of observation NT are equal to averaged characteristics on several implementations N in a short interval of time T. It means that the equality (for example, concerning assembly average) should be satisfied:

$$\frac{1}{NT}\int_0^{NT} x(t,\varphi_1)dt = \frac{1}{N}\sum_{n=1}^{N}\frac{1}{T}\int_0^{T} x(t,\varphi_n)dt \qquad (3)$$

where φ_n is a statistically distributed phase of the process $x(t)$.

According to (3), the assembly average (m_x) of 10 temporal implementations of a signal with an additive fractal structure in the time interval T_c differs from the m_x temporal implementation in the time interval $10T_c$ by $\varepsilon=0.00001$, which is an accuracy from which a series is considered to be ergodic.

For the quantitative estimation of a level of proximity of researched signals $W(t)$ to stochastic processes with the normal distribution law we use the fitting criterion of Kolmogorov q (Iglin, 2006). This criterion is based on a comparison of histograms of two processes.

Define a significance threshold $q=0.2$ and write down in one table all values of reference frequencies at which threshold excess is observed.

From Table 1 we can see that at certain values of the reference frequency by means of the Weierstrass function it is possible to simulate processes with the normal distribution law.

From the analysis it follows that application of the Weierstrass function as a fractal signal is

Figure 2. Spectrum plots of Weierstrass function (2) at λ=1.2

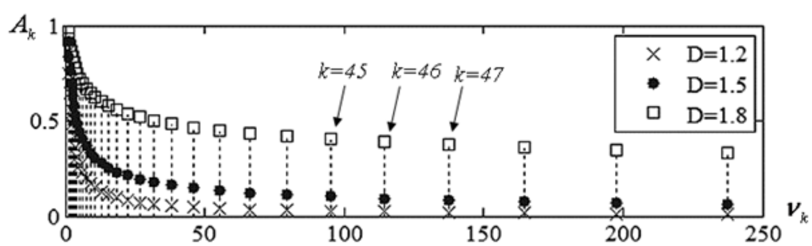

Box 1.

$$W(\lambda t) = \sum_{k=1}^{\infty}\lambda^{(D-2)k}\sin\left(\lambda\cdot\lambda^k t+\varphi_k\right) = \sum_{k=1}^{\infty}\lambda^{(D-2)k}\sin\left(\lambda^{k+1}t+\varphi_k\right) = \ldots$$

$$\ldots = \begin{Bmatrix} l = k+1 \\ k = l-1 \end{Bmatrix} = \sum_{l=2}^{\infty}\lambda^{(D-2)(l-1)}\sin\left(\lambda^l t+\varphi_l\right) = \frac{1}{\lambda^{(D-2)}}W(t)$$

that gives

$W(\lambda t)= \lambda^{(2-D)}W(t)$.

Table 1. Values of the reference frequencies for which the fitting criterion of Kolmogorov is more than 0.1

1,17	1,175	1,182	1,188	1,192	1,195	1,196	1,203	1,205	1,21
1,235	1,242	1,25	1,262	1,278	1,289	1,299	1,303	1,305	1,342
1,352	1,356	1,358	1,366	1,42	1,425	1,428	1,43		

complicated by two essential lacks following from its self-similarity and non-differentiability:

1. The complete series (2) occupies unfairly big frequency range.
2. The high non-uniformity distribution of energy on frequencies is observed. For example, for a signal on Figure 2 in initial area of frequencies from 0 to 25 Hz, occupying a small part from the general band, are concentrated 87% of all energy of a signal.

In following sections of this chapter the methods of elimination of these lacks are offered.

INCOMMENSURABILITY OF FREQUENCIES OF THE WEIERSTRASS ROW AS THE PRINCIPAL REASON OF AN IRREGULARITY OF ITS TEMPORAL IMPLEMENTATIONS

The important characteristic feature of the Weierstrass series (2) is that its components represent the sinusoidal functions with cyclic frequency λ^k. With k growth, cyclic frequencies of a series increase under the geometrical progression law (Figure 2), i.e. have the exponential growth. Moreover, frequencies of the Weierstrass series will be in an integer ratio extremely rarely (Kapranov & Khandurin, 2011, pp.23-26), only at certain values λ. It is an essential difference of the Weierstrass series from a Fourier series:

$$f\left(t\right)=\sum_{k=1}^{\infty}\omega^{\left(D-2\right)k}\sin\left(\omega k\cdot t\right),$$

in which all harmonics consist in an arithmetical progression with respect to ωk and (Figure 4) are multiple to the fundamental frequency.

It is clear that a ratio of frequencies of sinusoidal components of an additive series gives a periodicity of the function, and their exponential growth leads to a self-similarity. It is necessary to be very accurate during the selection of the λ value of the reference frequency. This parameter is responsible for incommensurability and for complexity (the absence of a regularity and periodicity, predictability, recurrence). At that, the incommensurability can be full or partial. At any values of parameter $\lambda\geq 2$ some periodicity is noticeable in behavior of the $W(t)$ function. It is important to mark the fact that if λ is an integer then the function (2) becomes completely periodical. This results from the fact that all frequencies of the Weierstrass series become multiple to

Figure 3. Comparison of the normalized histograms of distribution of a signal on the basis of the Weierstrass series W(t) on an observation interval T_c (black trace) and on an interval $10T_c$ (gray background). Parameters: D=1.9, λ=1.21

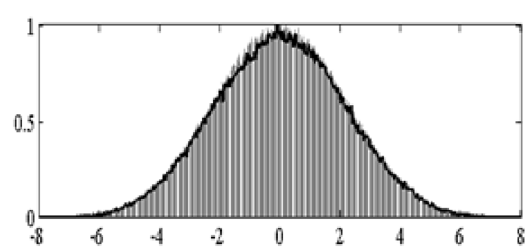

Figure 4. Comparison of additive series of Weierstrass (gray) and Fourier (black) at D=1.9, λ=ω=1.7. Normalized (a) temporal implementations, (b) spectrum plots.

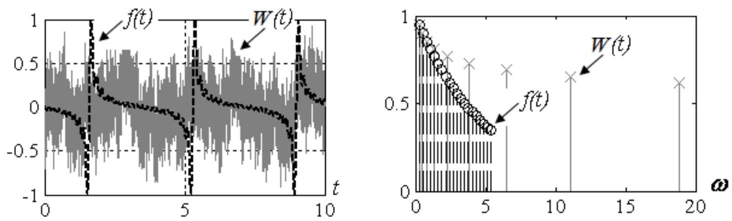

each other, the inherent incommensurability of frequencies disappears.

The forbidden values of the reference frequency are such values of λ_F for which there is a ratio condition (or commensurabilities) of two or more frequencies of the Weierstrass row *W(t)*,

$$m\lambda_F = \lambda_F^n$$

where *n=1,2,3 …, m=1,2,3, …* are integer numbers. From here we receive expression:

$$\lambda_F = \sqrt[(n-1)]{m} \qquad (4)$$

at *m=1* or *n=1* we have $\lambda_F=1$, and at *n=2* we have $\lambda_F=m$.

If a condition (4) is true, then the values of non-equidistant frequencies of the Weierstrass series can be obtained at an additive combination of several equidistant frequency grids. Number of such grids equals to *(n-1)* and among themselves their frequencies are not intersected (Figure 5). For example, at 11 members of the series *w(t)* and $\lambda_F=1$, we have a composition of two equidistant grids (with a number of frequencies 6 and 5, accordingly), and at $\lambda_F = \sqrt[3]{2}$ the number of such grids becomes three.

On the Figure 5 it can be seen that 12 members of the Weierstrass series with non-equidistant frequencies can be obtained by summation of three series with 8th equidistant frequencies in everyone (at given parameters).

If the condition (4) is not fulfilled, a Weierstrass series with non-equidistant frequencies cannot be made by an additive combination of series with equidistant frequencies. That is, if the reference frequency of the Weierstrass row does not concern the forbidden frequencies λ_F, all frequencies

Figure 5. Arrangement of frequencies on a geometrical and arithmetical progression. Parameters $\lambda = \lambda_R = \sqrt[3]{2}$.

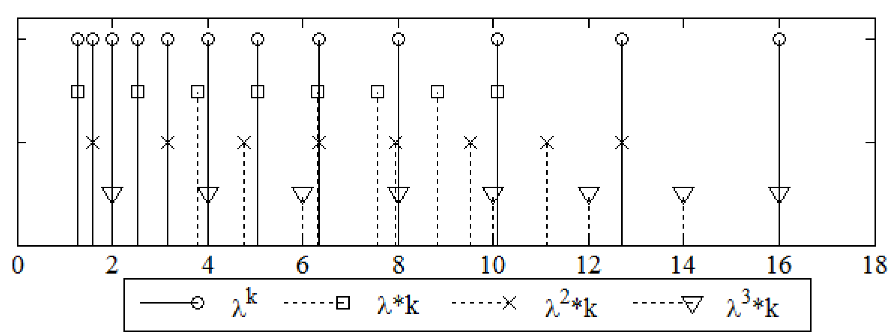

of such series have no general multiple and are completely incommensurable.

The best values for the reference frequency λ_0 need to be selected proceeding from a condition that they are located on the maximum distance from adjacent forbidden values λ_F. Thus, it is necessary to consider an accuracy ε from which we can set values λ_0, i.e.:

$$\lambda_0(n) = \frac{\lambda_F(n+1) + \lambda_0(n)}{2},$$

$$\text{at } \frac{\lambda_F(n+1) - \lambda_0(n)}{2} > \varepsilon. \tag{5}$$

Proceeding from (5) we can calculate values for the best frequencies (Table 2).

At an increase of the frequency accuracy ε, the number of the best values λ_0 dramatically increases – the more accuracy, the better incommensurability.

Proceeding from the calculated values of the forbidden and best frequencies, it is possible to select values λ under specific engineering tasks. For example, temporal implementations $W(t)$ with rather small number of members equal 4 show such behavior:

- If beat arises between all four frequencies, the full periodicity of temporal implementations is observed,
- If beat arises between two frequencies from four, the signal is quasi-periodical,
- If beat between series components' misses, the period of signal repetition is defined by a level of accuracy of signal's frequencies.

Thus, at already 4 members, but with well-selected value of λ, we obtain the very complicated signal. If the full incommensurability of frequencies is not important, such signal can be formed by means of an additive combination of several equidistant grids of frequencies.

TRUNCATION OF THE FREQUENCY BAND OCCUPIED BY SIGNALS WITH AN ADDITIVE FRACTAL STRUCTURE

To generate a radio signal on the basis of the Weierstrass function (2) it is necessary to pass from its mathematical note to technical interpretation. In other words, it is necessary to truncate a Weierstrass's series as in practice we have a possibility to form the restricted number of its members only. It can be done by different methods proceeding from the set of upper $f_H = \lambda^{k_H} / 2\pi$ and lower $f_L = \lambda^{k_L} / 2\pi$ boundaries of the selected frequency range:

$$w(t) = \sum_{k=k_L}^{k_H} \lambda^{(D-2)k} \sin\left(\lambda^k t\right), \tag{6}$$

where numbers of the first and last component of a truncated series $k_H > k_L > 1$. If we have selected a number of members of a series (6) $\Delta k = k_H - k_L$, then the parameter λ turns out equal to $\lambda = \sqrt[\Delta k]{f_H / f_L}$. On the other hand, having selected a specific value of λ, we can find the required number of series members $\Delta k = \ln\left(f_H / f_L - \lambda\right)$.

The relation $f_H / f_L = \lambda^{\Delta k}$ defines a frequency band occupied by a signal. The bandwidth essentially depends on the parameter λ. So at 50 members of a series of Weierstrass and $\lambda = 1.2$ the relation accepts the great value $f_H / f_L \approx 7583,7$. At insignificant magnification $\lambda \Rightarrow \lambda = 1.3$ the ratio increases by two orders $f_H / f_L \approx 383022,5$.

A truncated row of Weierstrass (6) possesses fractal properties only in a certain scale range. Besides, at passage from a complete Weierstrass series to the truncated one, there is the smoothing of its temporal implementation, i.e. a loss of complexity, the scale invariance and the dimensionality of the signal. At usage of fractal signals in secure communication systems, it is especially important to generate their as much as possible irregular and complex on the given interval of observation. Therefore, it is necessary to define a minimal number of members of a truncated series of Weierstrass *w(t),* at which losses in complexity would be minimal.

For an estimation of complexity of full (2) and truncated (6) signals, the numerical general-purpose measure is necessary. To use fractal dimension of oscilloscope patterns of these signals is expediently (Kapranov & Khandurin, 2011, pp.23-26) as such a measure. The method of calculation of the fractal dimension of temporal implementations of signals by means of creation of their structural functions (Korolenko & Maganova & Mesniankin, 2004) is convenient:

$$S_n = \frac{1}{K-n}\sum_{k=1}^{K-n}\left\|f_{k+n} - f_k\right\|,$$

where f_k is the analyzed function, time t is connected with an index $k=1,2,3,\ldots,K$ by a ratio $t = k\Delta t$, Δt is – the time slot between signal samples corresponds to the sampling rate.

Calculations of dimension D_{calc} show (Figures 6 and 7) that at number of members of truncated series (6) smaller than 10 and at the value of the reference frequency $\lambda=1.2$, the calculated dimension of the temporal implementation is almost equal to 1, at a magnification of a number of members of a series the dimension linearly increases and at $k_H>55$ is equal to theoretical dimension $D_{calc}=D=1.6$.

At a specific value of λ, the calculated dimension corresponds to theoretical dimension at a certain number of series members. For example, at $\lambda=1.2$ for achievement of the given dimension D it is necessary to take 55 members of a series minimum (Figure 7), and at $\lambda=1.7$ we need only 21 (Figure 7). However, if it is necessary to generate a signal on the basis of a truncated series of Weierstrass with the actual dimension of the temporal implementation equal to D_{calc} = 1.5, application 10 members of this series only is possible to set $D=1.8$ (Figure 7).

Figure 6. (a) Calculation of the signal dimension on the basis of a truncated series of Weierstrass depending on the number of members of a series for $D=1.6$, $k_L=1$, (b) temporal implementations of a signal at $k_H=20, 30, 50$

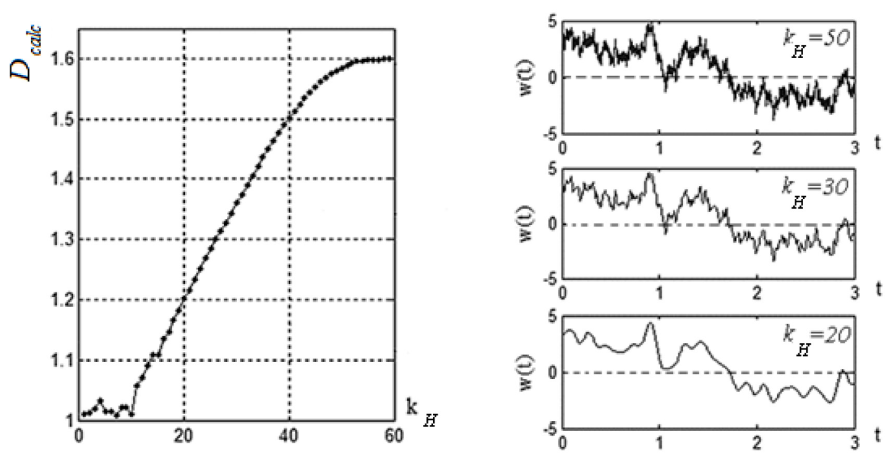

(a) (b)

THE FRACTAL SIGNAL ON THE BASIS OF WEIERSTRASS SERIES WITH A MODIFIED SPECTRUM

As it was shown above, the first lack of a signal on the basis of the truncated Weierstrass series (6) is the unfairly wide spectrum bandwidth. In the range of low frequencies its density is high, and in the range of high ones the spectrum is strongly rarefied (Figure 2). At that, the insignificant magnification of the parameter λ leads to a sharp increase of the frequency band occupied by a signal at an invariable number of its spectral components.

Let us consider the simple method allowing considerably compression of a spectrum, having saved thus the main advantages of a fractal signal structure (unpredictability, functional dependence of dimension of the graph of function $w(t)$ from parameter D), restriction of growth of the exponent k value of parameter λ both in the allocation of amplitudes, and in the law of arrangement of frequencies (Kapranov & Khandurin, 2011, pp.23-26). For this purpose we will enter new functional dependence with changeover

$$k \rightarrow \chi(m,k), \qquad (7)$$

where $\chi(m,k)$ is some function restricted on top, m is a frequency compression parameter. As a result of changeover (7), the initial truncated series (6) saves the formal structure, but there is absolutely other law of arrangement of amplitudes and frequencies $A_k^{\chi} = \lambda^{(D-2)\chi(m,k)}$, $\nu_k^{\chi} = \lambda^{\chi(m,k)}/2\pi$, than we get an expression:

$$w_{\chi}(t) = \sum_{k=k_{\min}}^{k_{\max}} \lambda^{(D-2)\chi(m,k)} \sin\left(\lambda^{\chi(m,k)} t\right). \qquad (8)$$

For example, we will select next limiting function $\chi\ (m, k)$:

$$\chi(m,k) = m \cdot th(k/m). \qquad (9)$$

From expression (9) it is clear that as $m \rightarrow \infty$, we obtain $\chi\ (m, k) \rightarrow k$.

In the Figure 8 characteristic of the relation of the upper frequency of a signal spectrum on the basis of the series (8) ν^{χ}_{H} to the upper signal frequency on the basis of the initial series (6) ν_H from compression parameter m is shown. It can be seen that parameter reduction m leads to essential compression of the frequency band occupied by a signal. As the law of compression (9) influences upon amplitudes of components of the series (8), then at a signal on its basis the law of spectrum recession is saved (Figure 8(b)).

Figure 7. Increment of the dimension D_{calc} of temporal implementations of w(t) caused by the growth of the number of its members. Parameters: k_{min}=1, (a) λ=1.2, (b) λ=1.8.

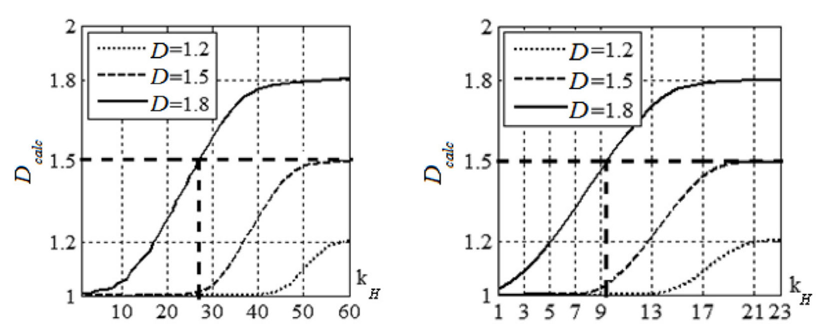

(a) (b)

From Figure 9(a) it is clear that the original signal frequency compression (up to very small m) does not influence on unpredictability of its temporal implementation. It happens because spectral components of the modified series (8) still are not multiple to each other, that is remained incommensurable.

At a limit of m=0 dimension of temporal implementation aspires to a minimum (Figure 9(b)). Comparing Figure 8(a) and Figure 9(b) we see that it is possible to allow frequency compression no more than 10 times at m=50 without reduction of the fractal dimension. The further reduction of the compression parameter m leads to dramatically reduction of the signal dimension at insignificant abbreviation of the frequency range. At technical implementation of the circuit, if it is not planned to use a dimension or self-similarity of a signal, it is possible to resolve the big level of compression.

THE FRACTAL SIGNAL ON THE BASIS OF THE ALIGNED WEIERSTRASS SERIES

The second lack of a concerned fractal signal is that the most part of its capacity is allocated far enough from assembly average. On other words, the mean value of the Weierstrass function strongly changes along an observation interval. In a signal constructed by the Weierstrass series with a truncated spectrum (6), more than 90% of capacity is allocated in less than 10% of the occupied frequency band, i.e. the frequency resource is spent too much ineffectively. To get rid of superfluous capacity and at the same time to extinguish spectral components of the Weierstrass series in the lower part of a spectrum, we will lead its centering concerning a current average.

For determination of the centered value of our series it is necessary to do the following operation:

$$w_C(t,\tau) = w(t) - M(t,\tau), \tag{10}$$

where $M(t,\tau)$ is a current average from the Weierstrass function in a window with width $\tau = 2\pi \big/ \lambda^{k_H - Z}$ ($Z=1 \ldots k_H$ is a number of high-frequency components of w (t), which are not subject to clearing), which is subtracted from an ordinary Weierstrass function (2). The current average from $w(t)$ is equal (see Box 2).

As a result, it is obtained a current average of the function $w(t)$,

$$M\left(t,\tau\right) = \sum_{k=1}^{\infty} \left[\frac{\sin(\tau\lambda^k/2)}{\tau\lambda^k/2} \right] \lambda^{(D-2)k} \sin(\lambda^k t), \tag{11}$$

Figure 8. (a) The level of frequency compression of a signal depending on m, (b) spectrum plots of signals on the basis of an initial series (6) and a series with frequency compression (8). Parameters for both series: D=1.8, λ=1.2 , k_L=1, k_H=50.

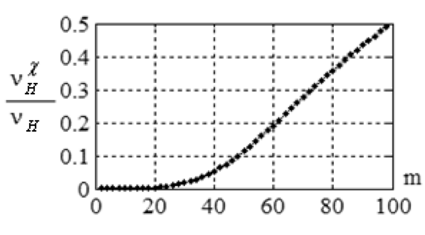

(a)

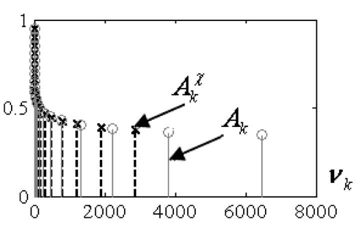

(b)

Figure 9. (a) Comparison of temporal implementations of signals on the basis of the initial truncated Weierstrass series (gray) and the series with modified spectrum (black) (m=40), (b) lowering of dimension of a series at frequency compression. Parameters of the series are similar to Figure 8.

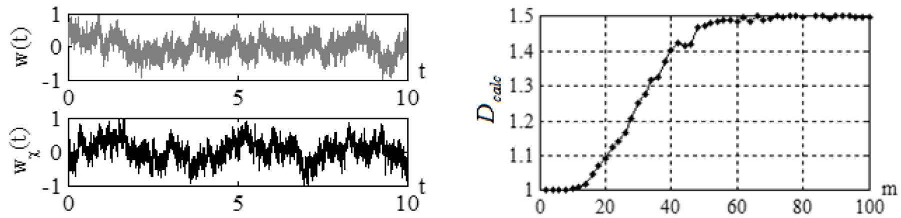

(a) (b)

Box 2.

$$M\left(t,\tau\right)=\frac{1}{\tau}\int_{\tau}^{t+\tau}w(t)dt=\frac{1}{\tau}\int_{t-\tau/2}^{t+\tau/2}\sum_{k=1}^{\infty}\lambda^{(D-2)k}\sin(\lambda^{k}t)dt=\frac{1}{\tau}\sum_{k=1}^{\infty}\left\{\lambda^{(D-2)k}\cdot\int_{t-\tau/2}^{t+\tau/2}\sin(\lambda^{k}t)dt\right\},$$

let us calculate expression under integral (weight factors of *k*-th component of a series),

$$\int_{t-\tau/2}^{t+\tau/2}\sin(\lambda^{k}t)dt=\frac{1}{\lambda^{k}}\left(\cos[\lambda^{k}(t-\tau/2)]-\cos[\lambda^{k}(t+\tau/2)]\right)=\frac{\sin(\lambda^{k}\tau/2)}{\lambda^{k}/2}\cdot\sin(\lambda^{k}t).$$

Table 2. The best values of the reference frequencies λ_0 for $\varepsilon=10^{-3}$

1,085	1,097	1,113	1,126	1,139	1,158	1,168	1,180
1,193	1,198	1,210	1,222	1,232	1,244	1,248	1,255
1,268	1,284	1,294	1,301	1,306	1,312	1,325	1,332
1,337	1,343	1,347	1,356	1,363	1,366	1,374	1,381
1,385	1,388	1,393	1,399	1,406	1,412	1,415	1,420
1,428	1,433	1,439	1,444	1,447	1,451	1,456	1,461
1,466	1,474	1,478	1,482	1,490	1,492	1,497	1,501
1,505	1,508	1,518	1,521	1,525	1,528	1,532	1,539
1,543	1,546	1,550	1,556	1,562	1,566	1,569	1,572
1,578	1,583	1,589	1,594	1,597	1,599	1,607	1,612
1,617	1,621	1,624	1,628	1,637	1,652		

Having substituted in (10) expressions for a truncated series *w(t)* (6) and its current average *M(t)* (11), we will obtain a note of the truncated aligned series of Weierstrass:

$$w_{C}(t,\tau)=\sum_{k=k_L}^{k_H}\left(1-\frac{\sin\left(\tau\lambda^{k}/2\right)}{\tau\lambda^{k}/2}\right)\lambda^{(D-2)k}\sin(\lambda^{k}t),\qquad(12)$$

where the law of arrangement of amplitudes and frequencies is $A_{k}^{C}=\left(1-\frac{\sin\left(\tau\lambda^{k}/2\right)}{\tau\lambda^{k}/2}\right)\lambda^{(D-2)k}$, $\nu_{k}^{C}=\nu_{k}=\lambda^{k}/2\pi$.

Graphs in the Figure 10 visually show a convenience of usage of the aligned function $w_C(t,\tau)$ instead of an original function of Weierstrass

$w(t,\tau)$. If a dynamic range of an original function is wide (it is noticeable even on a small interval of time of the observation presented on the Figure 10(a)) the range of change of the aligned function $w_C(t,\tau)$ is reduced by the order. That is especially important at formation wideband carrying oscillations on the basis of fractal function for transmission of information signals.

In the Figure 10(b) a characteristic of the relation of energies (calculated under the formula $E_f = \int_0^{Tc} f(t)^2 dt$, where T_c is a duration of temporal implementation) of signals on the basis of the aligned series (12) and the original series (6) from parameter Z defining a width of a window of selection of a current average. It is clear that energy of the aligned function decreases proportionally to Z^{3-D}. So at the high dimension of temporal implementation $D\to 2$ characteristic assumed to be linear (in the Figure 10(b) it is shown by a gray dotted line) and energy of a signal will decay in direct ratio to a number of not aligned components of the series Z. But with reduction of D the scoring from aligning operation sharply increases, apparently in the Figure 10(b) even at great value $Z=40$ the energy of the aligned series for $D=1.4$ is reduced by five times in relation to the not aligned.

As to a level of complexity of the aligned function $w_C(t,\tau)$ (the dimension of its temporal implementation), at correctly selected width of a window τ it is not much above, than complexity of an original function $w(t)$. Principal difference is that oscillations $w_C(t,\tau)$ does not contain slowly changing components as in its spectrum the low-frequency components are removed. Apparently from Figure 10(c) at reduction Z, i.e. at reduction of width of a window of integration τ, the magnification of dimensionality of temporal implementation from set to maximum $D_{calc}\to 2$ is observed. On the graph it is possible to select the critical value Z_{crit}, which indicates that dimension of a signal is always equal 2.

Figure 10. (a) Temporal implementations of signals on the basis of series (6, 11, 12) at D=1.8, λ=1.2, Z=20, (b) reduction of energy and (c) magnification of dimensionality of temporal implementation of a signal on the basis of the aligned series (12) at reduction Z

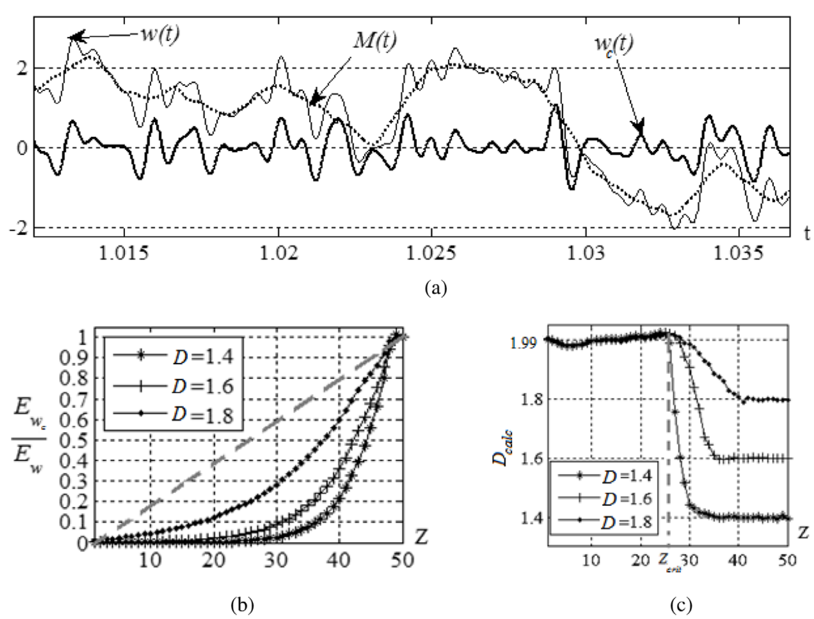

Comparing characteristics of the Figure 10(b) and the Figure 10(c) it is possible to draw an output that application of operation of an aligning to fractal signals with small dimension of temporal implementations $D < 1.5$ leads to the strong reduction of their energy at dimension minor change.

Spectrum plots of signals (Figure 10(a)), are resulted on the Figure 11 at the same values of parameters, as on Figure 10(a). Daggers mark amplitudes of spectral components of an original function $w(t)$, the circles – the aligned function $w_C(t,\tau)$.

In Figure 11 we see the strong suppression of a spectrum of $w_C(t,\tau)$ in the field of low frequencies and its riches in the field of high frequencies. It is possible to tell that oscillations of the aligned function, which are exceeding frequency of the full clearing $1/\tau = \lambda^{kH - Z}/2\pi$, have some power growth.

Having eliminated limitation of fractal signals on the basis of the Weierstrass series, it is possible to pass to experiments on stealthiness transmission of voice messages.

EXPERIMENTS ON TRANSMISSION OF THE VOICE SIGNALS BY MEANS OF FRACTAL SIGNALS ON THE BASIS OF WEIERSTRASS SERIES

In the present chapter we pose a task on secured transmission of the sound message masked by a fractal signal, by means of acoustic waves. For simplification of circuits of the receiver and the transmitter the voice should not be exposed to digitization. Masking and its removal should happen in real time. A level of stealthiness of transmission and quality of signal demodulation is defined as visually, by comparing of oscilloscope patterns of the initial message with demodulated one, and on hearing the results. The first method of cleaning up of the information message from the masking is based on precision of fractal signals on the basis of $w(t)$.

The Coherent Elimination of the Masking Fractal Signal in the Receiver

Thanks to high reproducibility of fractal signals, it is possible to implement a communication system with fractal masking in the transmitter and the coherent elimination of this masking (Figure 12). Here voice message masking was led as a signal on the basis of a truncated Weierstrass series (6), and a signal on the basis of a series with the compressed spectrum (8).

In computational experiments the information voice message $s(t)$ represents a remark “This information is confidential, absolutely confidential” duration 4.004sec and occupies the frequency band from f_L=105Hz to f_H=2000Hz, a sampling rate has been selected from the computer equal to f_S=44100Hz. As masking oscillations, the signal on the basis of a truncated series of Weierstrass

Figure 11. Spectrum plots of the aligned series of Weierstrass (parameters are similar to Figure 10) (a) Z=3, (b) Z=10

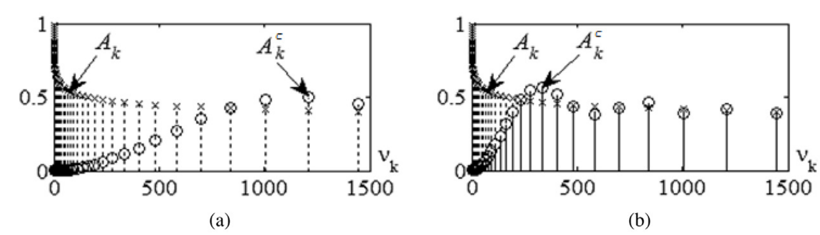

(6), with parameters $D=1.9$, $\lambda=1.15$, $k_L=52$, $k_H=71$, thus the lower signal frequency $f_L=228Hz$ and upper $f_H=3246Hz$ has been used. Frequency bands of information and masking signals were commensurable and were superimposed that was saved and at frequency compression.

It has appeared that quality of masking and demodulation in the given circuit is very high, it has proved to be true in experiment at message listening in the communication channel and on a receiver output. In a vocal range of frequencies humans clearly distinguish the separate spectral components about accuracy to hertz, besides the human ear possesses high sensitivity, i.e. at signal power reduction in 1000 times it seems to us that power level has decreased only 30 times. However, if to mask the sound message a fractal signal on hearing it will cease to be recognized. Probably, it is connected to hearing aid singularities.

In the given circuit implementation of the unit of synchronization of the fractal generator in the receiver appears too difficult. For simplification of the receiver circuit the structure with incoherent removal of a mask from a signal is offered.

Incoherent Elimination of a Masking Fractal Signal in the Receiver

In (Kapranov & Khandurin, 2009, pp.89-92) the system of secured communication FRAMASK with incoherent reception and information message, masking by a fractal signal in the transmitter is offered. This system is similar on the structure to a communication system at chaotic masking (Murali, Leung, & Yu, 2003, pp.432-441), but in it fractal signals are used as difficult carrier oscillations (Figure 13) instead of chaotic. Window operation of the moving average is applied to support a secrecy of transmission on the transmitting and receiving sides. Thanks to application of fractal maskers and the multistage moving average in the receiver for selection of the information message in this circuit, unlike the circuit with chaotic signals, the high secrecy of transmission of the message and high quality of demodulation can be reached, at information transfer through the communication channel with additive noises.

In the transmitter (Figure 13) the analog message $s(t)$ is additive combined with a masking

Figure 12. (a) System of secure communication with fractal masking in the transmitter and the coherent reception. Temporal implementations: (b) the sound message s(t), (c) the disguised message r(t), (d) messages on a receiver output e(t).

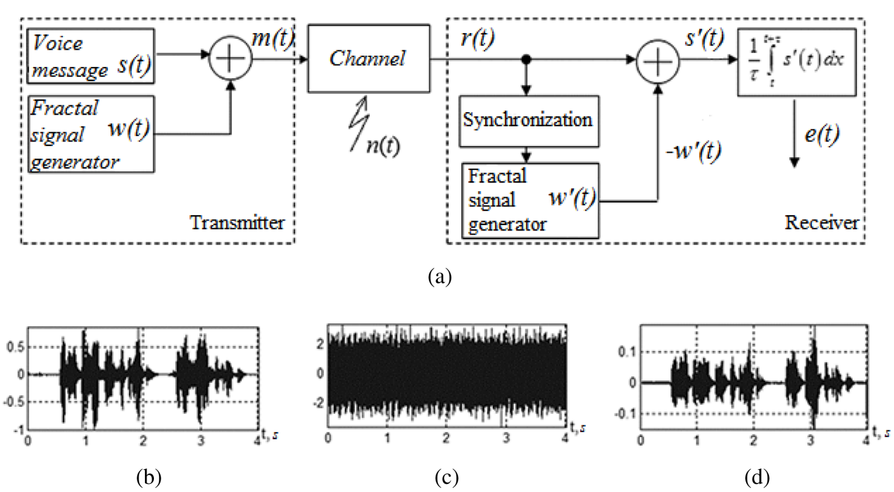

fractal signal on the basis of *w(t)*, processed by centering operation. On the reception side there is a multistage operation of the moving average, permitting at the expense of ergodicity of the aligned series to remove masking and to get rid of noise.

As a result, temporal implementation of a signal on an output of the incoherent receiver (Figure 13) is strongly distorted, however, at hearing the voice message is quite legible.

Low quality of separation of information from masking oscillations in the considered circuit (Figure 13) is caused by necessity of the strong level reduction of the sound message for secure transmission at communication channel, but this reduction degrades a quality of separation of the initial message from masker. To refine the quality of demodulation at high secrecy, the method of change of the circuit on Figure 13 consisting of two stages is developed. The first stage is an adaptation of a spectrum of a fractal signal to a spectrum of the message for improving of its masking properties.

A number of experiments on masking of the sound message by fractal signals with frequency compression of a type (8) have been fulfilled. Functional schemes of systems with such signals are similar to the system shown on Figure 12, but the generator of the fractal signal with a compressed spectrum with parameters was used here: $D=1.9$, $\lambda=1.15$, $k_L=33$, $k_H=52$, thus, the lower signal frequency is $f_L=201Hz$ and upper $f_H=201Hz$. The signal spectrum is compressed under the law $\chi(k,m) = mk\left[1-\left(2k/3k_{\max}\right)^4\right]$, where $m=1.6$.

It has been obtained that quality of masking of information for a signal on the basis of $w_\chi(t)$ is better, than for a signal on the basis of an original series *w(t)* at the identical power level *s(t)*. However. In this case, masking is too good, cleaning up of the message from a mask by its multistage window moving average appears to be impossible.

Figure 13. (a) System of secure communication with fractal masking and window moving average in the transferring and receiving sides; temporal implementations: (b) the sound message s(t), (c) the disguised message r(t), (d) messages on a receiver output e(t)

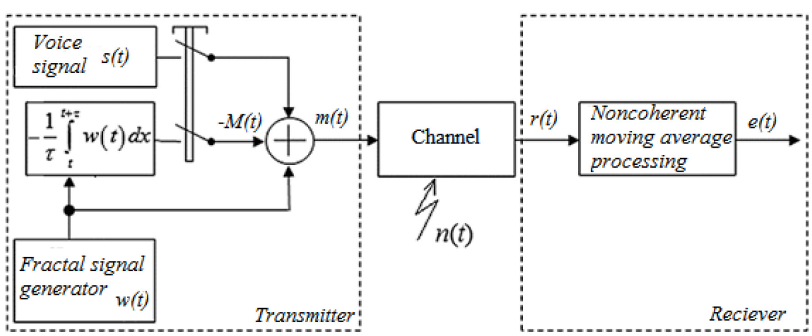

(a)

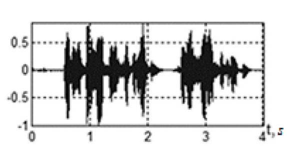

(b)

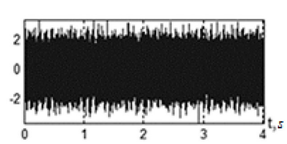

(c)

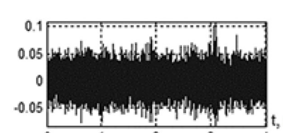

(d)

To define a presence of the secured message on an input and a demodulator output is not possible visually and during a hearing.

The second stage of modification of the original circuit (Figure 13(a)) consists in a failure from centering operation on the transmitting end (Figure 14). In the circuit on Figure 14 the parameters of masker are following: $D=1.9$, $\lambda=1.15$, k_{L1} =52, k_{L2}=62, k_H=71, the frequency compression law at an open-ended key the lower signal frequency is $f_{L1}=228Hz$, and at shorted $f_{L2}=923Hz$ and the upper frequency is f_H $=1796Hz$. Signal demodulation was produced similarly as it is in the original circuit. At the appearance of the sound message on a transmitter input, the electronic key is shorted, thus, the generator of a fractal signal ceases to form those components of series $w_\chi(t)$, which were superimposed with a spectrum of the appeared message. At such operation the secrecy of transmission of the message does not decrease, but quality of demodulation increases, temporal implementations are similar Figure 13(b)-(d).

Thus. In the given section two methods of transmission of the voice messages disguised by a fractal signal with additive structure from listening by the third party are developed. The first method is based on the coherent subtraction of masker from the accepted. Circuit implementation of the receiver in such a system is difficult – it is necessary to construct the generator of a fractal signal identical to the generator of the transmitter and to have the unit of its synchronization. However, in this case, there is a quasi-optimal reception of a signal, i.e. their full cleaning up from masking oscillations. The second method is based on incoherent processing of an accepted signal for removal from it the masking fractal oscillations and a white noise. The communication system constructed under such circuit possesses simple implementation of the receiver and does not concede to coherent system on quality of extraction of information.

FUTURE RESEARCH DIRECTIONS

The developed methods of information transfer by means of signals with an additive fractal structure are based only on their high level of reproducibility and wideband. In the further publications we are going to make experiments on usage of self-similarity of these signals, for improvement of quality of demodulation on the receiving side. Also a perspective direction of research is the dimension modulation of temporal implementations of signals with an additive fractal structure.

A number of experiments on direct fractal information transmission by means of signals of a new type have been fulfilled. In such method of the transmission the binary information sequence is multiplied with carrying fractal oscillations, and in the receiver there is an energetic detection

Figure 14. System of secure communication with fractal masking in the transmitter and the window moving average on the receiving side

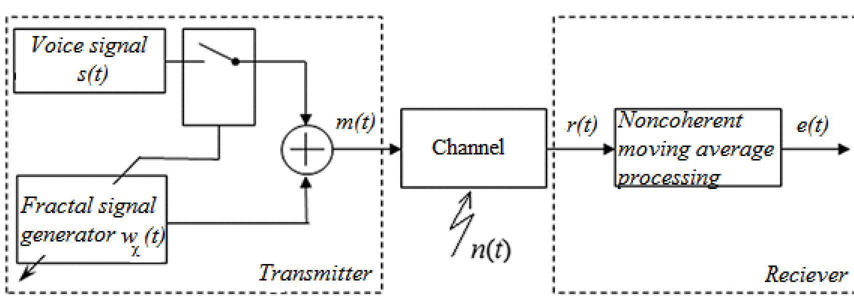

of the received wideband pulses. Researches in the given direction are perspective as such communication systems correspond to the standard of communication IEEE 802.15.4a (UWB).

Besides, it is necessary to develop circuits of generators of offered signals.

CONCLUSION

As a result of this chapter, the following main conclusions are obtained:

- Complex wideband signals with an additive fractal structure on the basis of a series of Weierstrass possess a number of singularities (self-similarity, non-differentiability and precision) and can be used in radio engineering applications.
- Methods of modification of probed fractal signals for more effective expenditure by them of frequency-power resources are offered. Therefore, have been entered into reviewing a fractal signal with a compressed spectrum and the aligned fractal signal. Conditions, at which there is no loss of complexity of original signals at passage to the modified, are found.
- Experiments on reserved transmission of a voice message by means of fractal signals on a communication channel with a white noise are made. Two transmission schemes of the information by means of a new type of signals are developed.

REFERENCES

Bolotov, V. N., & Tkach, Y. V. (2006). Generating of signals with a fractal spectra. *Journal of Technical Physics*, *76*(4), 91–98.

Cuomo, K. M., & Oppenheim, A. V. (1993). Circuit implementation of synchronized chaos with applications to communications. *Physical Review Letters*, *71*(1), 65–68. doi:10.1103/PhysRevLett.71.65 PMID:10054374.

Dedieu, H., Kennedy, M. P., & Hasler, M. (1993). Chaos shift keying: modulation and demodulation of a chaotic carrier using self-synchronizing Chua's circuits. *IEEE Transactions on Circuits and Systems II*, *40*, 634–642. doi:10.1109/82.246164.

Dmitriev, A. S., & Panas, A. I. (2002). *Dynamic chaos: New information carriers for communication systems*. Moscow, Russia: Fizmatlit.

Du Bois, & Reymond, P. (1875). Verch einer classification der willrurlichen functionen reeler argumente nach ihren aenderungen inden beinsten intervallen. *Journal Furder Reine und Angewandte Mathematiques*, *79*, 21–37.

Falconer, K. J. (1997). *Techniques in fractal geometry*. New York: John Wiley & Sons.

Gluzman, S., & Sornette, D. (2002). Log-periodic route to fractal functions. *Physical Review Letters E*, *6503*(3), 418–436.

Iglin, S. P. (2006). *Probability theory and the mathematical statistics on the basis of MATLAB: The manual*. Kharkov, Ukraine: NTU.

Ipatov, V. (2007). *Wideband systems and CDMA: Principles and applications*. Moscow, Russia: Technosphera.

Kapranov, M. V., & Khandurin, A. V. (2009). Information transmission with fractal masking (framask) in communication system [in Russian]. *Vestnik MPEI*, *1*, 89–92.

Kapranov, M. V., & Khandurin, A. V. (2011). Signals with additive fractal structure for information transmission. *Journal of Electromagnetic Waves and Electronic Systems*, *16*(2), 23–36.

Kapranov, M. V., & Morozov, A. G. (1998). Application of chaotic modulation for information transfer. *Radiotechnicheskie Tetrady*, *14*, 66–71.

Kapranov, M. V., & Tomashevsky, A. I. (2003). System of secure communication with usage of correlative reception and the synchronous chaotic response. *Journal of Electromagnetic Waves and Electronic Systems*, *8*(3), 35–48.

Korolenko, P. V., Maganova, M. S., & Mesniankin, A. V. (2004). *Innovation methods of the analysis of stochastic processes and structures in optics: Fractal and multiracial methods, wavelet-conversions: The manual*. Moscow, Russia: MSU, Nuclear Physics, Scientific Research Institute.

Kravchenko, V. F., Perez-Meana, H. M., & Ponomaryov, V. I. (2009). *Adaptive digital processing of multidimentional signals with applications*. Moscow, Russia: Fizmatlit.

Kuznetsov, S. P. (2000). *Dynamic chaos (lecture course)*. Moscow, Russia: Nauka.

Murali, K., Leung, H., & Yu, H. (2003). Design of noncoherent receiver for analog spread-spectrum communication based on chaotic masking. *IEEE Journal*, *50*(3), 432–441.

Pecora, L. M., & Carroll, T. L. (1990). Synchronization in chaotic systems. *Physical Review Letters*, *64*, 821–824. doi:10.1103/PhysRevLett.64.821 PMID:10042089.

Tomashevsky, A. I., & Kapranov, M. V. (2006). Fractal properties of chaotic dynamic processes in reverse time. *Nonlinear World*, (4-5), 214–237.

Wornell, G. (1996). *Signal processing with fractals: A wavelet-based approach*. London, UK: Prentice-Hall International.

Yang, T. (2004). A survey of chaotic secure communication systems. *International Journal of Computational Cognition*, *2*(2), 81–130.

ADDITIONAL READING

Arnold, V. I., Afraimovich, V. S., Il'yashenko, Yu. S., & Shilnikov, L. P. (1999). *Bifurcation theory and catastrophe theory*. New York: Springer.

Belykh, V. N., & Chua, L. O. (1993). A new type of strange attractor related to the Chua's circuit. *Journal of Circuits*. *Systems and Computers*, *3*(2), 361–374.

Berry, M. V., & Lewis, Z. V. (1980). On the Weierstrass-Mandelbrot fractal function. *Proceedings of the Royal Society of London. Series A*, *370*, 459–484. doi:10.1098/rspa.1980.0044.

Bogolyubov, A. N., Koblikov, A. A., & Shapkina, N. E. (2009). Fractal electrodynamics: Analysis and synthesis of fractal antenna radiation pattern. In *Proceedings of PIERS*, (pp. 879-882). PIERS.

Chalice, D. R. (1991). A characterization of the cantor function. *The American Mathematical Monthly*, *98*, 255–258. doi:10.2307/2325032.

Falconer, K. J. (1990). *Fractal geometry: Mathematical foundations and applications*. New York: John Wiley & Sons.

Farmer, J. D., Ott, E., & Yorke, J. A. (1983). The dimension of chaotic attractors. *Physica D. Nonlinear Phenomena*, *7*(1), 153–170. doi:10.1016/0167-2789(83)90125-2.

Felber, P. (2000). *Fractal Antennas*. Chicago: Illinois Institute of Technology.

Grassberger, P., & Procaccia, I. (1983). Characterization of strange attractors. *Physical Review Letters*, *50*(5), 346–349. doi:10.1103/PhysRevLett.50.346.

Halle, K. S., Wo, C. W., Itoh, M., & Chua, L. O. (1993). Spread spectrum communication through modulation of chaos. *International Journal of Bifurcation and Chaos in Applied Sciences and Engineering*, *2*, 469–477. doi:10.1142/S0218127493000374.

Hardy, G. H. (1916). Weierstrass's non-differentiable function. *Transactions of the American Mathematical Society*, *17*, 302–323.

Hunt, B. R. (1998). The Hausdorff dimension of graphs of Weierstrass Function. *Proceedings of the American Mathematical Society*, *126*(3), 791–800. doi:10.1090/S0002-9939-98-04387-1.

Kocarev, L., Halle, K. S., Eckert, K., Chua, L., & Parlitz, U. (1992). Experimental demonstration of secure communications via chaotic synchronization. *International Journal of Bifurcation and Chaos in Applied Sciences and Engineering*, *3*, 709–713. doi:10.1142/S0218127492000823.

Kolumban, G., & Kennedy, M. P. (1998). The role of synchronization in digital communications using chaos: Part II–Chaotic modulation and chaotic synchronization. *IEEE Transactions on Circuits and Systems. I, Fundamental Theory and Applications*, *45*, 1129–1140. doi:10.1109/81.735435.

Leland, W. E., Taqqu, M. S., Willinger, W., & Wilson, D. V. (1994). On the self-similar nature of ethernet traffic. *IEEE/ACM Transactions on Networking*, *2*(1), 1–15. doi:10.1109/90.282603.

Li, T., & Yorke, J. A. (1975). Period three implies chaos. *The American Mathematical Monthly*, *82*, 985–992. doi:10.2307/2318254.

Lorenz, E. (1963). Deterministic non-periodic flows. *Journal of the Atmospheric Sciences*, *20*, 130–141. doi:10.1175/1520-0469(1963)020<0130:DNF>2.0.CO;2.

May, R. M. (1976). Simple mathematical models with very complicated dynamics. *Nature*, *261*, 459–467. doi:10.1038/261459a0 PMID:934280.

Park, K., & Willinger, W. (2000). *Self-similar network traffic and performance evaluation*. New York: John Wiley & Sons. doi:10.1002/047120644X.

Parlitz, U., Chua, L., Kocarev, L., Halle, K., & Shang, A. (1992). Transmission of digital signals by chaotic synchronization. *International Journal of Bifurcation and Chaos in Applied Sciences and Engineering*, *4*, 973–977. doi:10.1142/S0218127492000562.

Peitgen, H. O., Jurgens, H., & Saupe, D. (1992). Fractals for the classroom. In *Introduction to Fractals and Chaos*. New York: Springer. doi:10.1007/978-1-4757-4740-9.

Potapov, A. A., & German, V. A. (1998). Detection of artificial objects with fractal signatures. *Pattern Recognition and Image Analysis*, *8*(2), 226–229.

Raghavendra, B., & Dutt, D. (2010). Computing fractal dimension of signals using multiresolution box-counting method. *International Journal of Engineering and Mathematical Sciences*, *6*, 50–65.

Rocco, A., & West, B. J. (1998). Fractional calculus and the evolution of fractal phenomena. *Physica A*, 535–546.

Rossler, O. E. (1976). An equation for continuous chaos. *Physical Review Letters*, *57A*(5), 397–398.

Sharkovsky, A. N. (2006). Ideal turbulence. *Nonlinear Dynamics*, *44*, 15–27. doi:10.1007/s11071-006-1931-7.

Voss, R. F., & Clarke, J. (1975). 1/f noise in music and speech. *Nature*, *258*, 317–318. doi:10.1038/258317a0.

Yang, X., & Chiochetti, J., Papadopoulos, & Susman, L. (1999). Fractal antenna elements and arrays. *Applied Microwave & Wireless*, *5*, 34–46.